A Compact, Lightweight Sensor to Measure Bearing Angle to a Radio Transmitter

Liangchun Xu, *Tufts University*

BIOGRAPHY

Liangchun Xu is a Mechanical Engineering Ph.D. candidate at Tufts University in Medford, Massachusetts. He received his B.Eng. and M.Eng. in Geomatics Engineering from Wuhan University, China, in 2012 and 2014, respectively. Currently he works in the Automated Systems and Robotics Lab (ASAR) under Professor Jason Rife.

ABSTRACT

This paper describes a novel compact, lightweight sensor to measure the bearing angle to a radio transmitter. The proposed angle-of-arrival (AoA) sensor consists of a flat antenna array, which is composed of dipole and loop antenna elements. The dipole and loop antennas are quite small in size compared with the wavelength of the sensor's operating frequency. Therefore, the proposed antenna array is compact and very tolerant to manufacturing error (since antenna elements do not operate at their excitation frequency). The AoA estimate is obtained from signal magnitude measurements at each antenna element. A look-up table is employed to invert the bearing angle of the incoming signal given the observed signal magnitude at each antenna element. A sensitivity study indicates that the sensor performs well as long as the overall system design, including signal processing, delivers a signal-to-noise ratio (SNR) exceeding 42 dB.

INTRODUCTION

Angle of Arrival (AoA) sensing has potential to enable or augment positioning and orientation in GPS denied environments [1]. As one application, consider an emergency response scenario, such as rescuing survivors from a burning building. Usually the victim's absolute position can't be obtained through GPS directly because of the signal blockage in indoor environment. If the relative AoA information between the victim and rescuer can be obtained through mobile communication, the firefighter is much more likely to find the victim. As the firefighter approaches the victim, received signal power increases and the precision of AoA measurements grows higher. Other possible applications of compact, lightweight, and networked AoA sensors include tunnel navigation, package tracking, and augmented reality.

To address these potential applications, an AoA sensing system based on one-way radio broadcasts (transmitter to receiver) is envisioned. Unfortunately, available off-the-shelf AoA sensors are too large and costly to embed in a mobile phone. Many existing AoA sensors rely on phased antenna arrays that interfere signals to solve for the array orientation. Examples of small devices (below 1 m in their longest dimension) include [2, 3]. Off-the-shelf sensing systems that rely on reflected signals are also available (e.g. radar and lidar [4, 5]), but these devices are generally power hungry; moreover, they cannot identify targets uniquely, as is possible with a one-way broadcast from a uniquely-coded transmitter.

To fill the technology gap, this paper will develop a small, flat antenna array specifically designed to determine AoA. To keep processing and calibration as simple as possible, our antenna will rely primarily on measuring signal magnitude (and not phase) for the arriving signal. This approach contrasts with many existing direction finding (DF) technologies, such as Very High Frequency (VHF) Omnidirectional Radio Range (VOR) in aviation [6], space-time adaptive processing for beam steering [7, 8], or distributed-array systems enabled by complex spectrum estimation algorithms such as MUSIC or ESPRIT [9, 10]. Our approach of excluding phase measurements and relying on signal magnitude measurements represents some loss of information, but greatly simplifies calibration and processing as compared to these existing methods. Moreover, the flat form factor of the proposed device is well-suited for integration into mobile phones and other consumer devices.

The remainder of this paper details the proposed sensor design. First, requirements of the target AoA sensor are quantified. Next, based on these requirements, a novel compact, lightweight AoA sensor design is presented, including both the antenna design and corresponding AoA estimation algorithm. Finally, simulations are used to evaluate sensor performance in relation to our motivating application (i.e., emergency response).

SYSTEM REQUIREMENTS

To quantify system requirements for the AoA sensor to be built, we consider a first-response scenario. In this scenario, it is assumed that a victim is located in a building and that the victim's cell phone can broadcast an omnidirectional radio signal. The first responders are assumed to be equipped with compact AoA sensors (smaller than $10\ cm \times 10\ cm$), capable of receiving the broadcast from the victim. Since the transmitter (and possibly the receivers) are assumed to be embedded in mobile phones, the carrier signal for the broadcast is assumed to be 2.4 GHz. Considering the speed of the rescuers, a 1 Hz output frequency is reasonable. It is expected that the AoA sensor can provide 3D AoA measurements, to help perform direction finding in a structure with multiple floors.

As for the angular measurement accuracy, the effects of angular error are largest when the rescuers are farthest away from the victim. For our purposes, we will envision that the worst-case scenario puts the rescuers at a distance of 100 m from the victim, and that the rescuers need to distinguish on which floor the victim is located (assuming height between floors is about 3 m). Fig. 1 describes the geometry of this scenario. Using small angle approximation, the angle measurement error β should be less than about $\tan^{-1}\frac{3}{100} = 1.72$ degrees accordingly. Though high integrity is also relevant for this first-response scenario, this paper will consider only sensor accuracy, leaving an integrity analysis for future work.

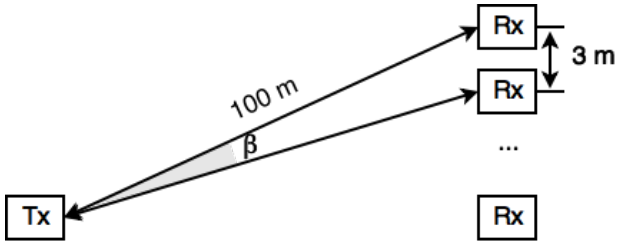

Fig.1. Geometry analysis for angular error quantification

While the above requirements are derived with a first-response scenario in mind, the same requirements would also serve well in other applications of interest (including tunnel navigation, etc.).

SYSTEM DESIGN

A novel AoA sensor design is proposed in this section. The sensor design comprises both a flat antenna array and an estimation algorithm that converts signal magnitudes received by array elements into an AoA measurement.

In this paper, we have intentionally focused on the receiver antenna array, treating the transmitter as an omnidirectional radio broadcast. In the longer term, we envision operating the antenna array as a transceiver, with both a receive and transmit capability. This future vision will allow for mutual direction-finding among all parties sharing AoA measurements, for instance as described in [11].

Receiver Antenna Array

To ensure a form factor compatible with integration in a consumer electronic device (for instance in a cell phone), we envision a planar antenna. In this paper, we specifically focus on a flat antenna array composed of five elements on one plane, including a small loop antenna and four short dipoles around it as shown in Fig. 2. The dipoles are configured symmetrically about the center of the loop in a square pattern. The nominal length of each dipole element is $\frac{1}{16}$ wavelength of the operating frequency 2.4 GHz, which is 7.8 mm. The circumference of the loop is $\frac{1}{20}$ wavelength of the operating frequency, which is 6.2 mm . The dipoles are displaced from the center of the loop antenna by a distance 4.7 mm. Feeders are identified in Fig. 2 as small dots. The feeder for each dipole is located at the dipole's center, and the feeder for the loop is located at one of the four points on the loop closest to a dipole antenna. The offset of the loop antenna's feeder is the only asymmetry in the design, but the effect of this asymmetry is extremely minor.

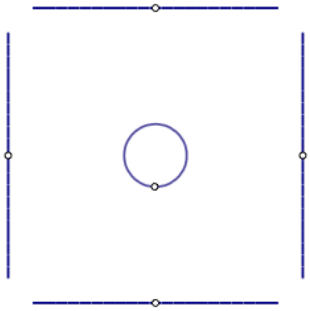

Fig. 2. Antenna design

The proposed AoA sensor extracts five independent received signal magnitude measurements, one from each of the five antennae. By design, the antenna elements are complementary, so that information is available to describe AoA in terms of an azimuth angle ϕ (angle of transmitter in the plane of the antenna) and an elevation angle θ (angle out of the plane of the antenna), as illustrated in Fig. 3. Information about the transmitter's azimuth angle can be inferred by comparing the signal power on orthogonal dipole antennae, as the dipoles each have a null along their own axes. Information about the transmitter's elevation angle can be inferred by comparing the signal power received by the dipole antennae to the loop antenna, since the combined dipoles provide a strong out-of-plane gain, whereas the loop antenna has a null orthogonal to the loop. To understand these relationships between AoA and gain pattern better, it is necessary to compute the antenna radiation pattern associated with each element (i.e. each feeder) in the system.

The radiation pattern is determined by the antenna's size and construction. In this paper, an open source program called Numerical Electromagnetics Code (NEC) is used to calculate radiation pattern for the proposed antenna array [12]. The NEC package is configured to compute the transmit pattern for an antenna, but by the principle of reciprocity, the transmission gain pattern is equivalent to the reception gain pattern. The code automatically accounts for mutual coupling among antenna elements.

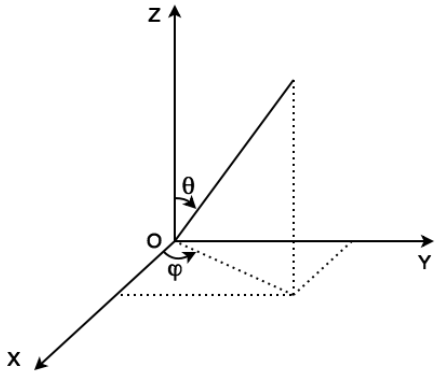

Fig. 3. Spherical coordinates

Because of the symmetry in the system, radiation patterns were evaluated for the loop antenna and only two of the dipoles (the leftmost and topmost dipoles shown in Fig. 3). Although NEC computes a 3D gain pattern over all azimuth and elevation angles, it is somewhat difficult to visualize this 3D pattern on the printed page. Instead, slices through the gain patterns are shown here in two planes, the azimuth plane (Fig. 4) and the elevation plane (Fig. 5). Here the azimuth plane is defined as the plane parallel to the **x** and **y** axes and passing through the origin (as shown in Fig. 3). Here the elevation plane is defined as the plane parallel to the **y** and **z** axes and passing through the origin. The radiation pattern for each antenna is shown in polar coordinates, where the radius indicates antenna gain as a function of angle (azimuth angle in Fig. 4 and elevation angle in Fig. 5). Gains are plotted on a dB scale, with all values below a minimum (-30 dB) mapped to the center point.

For visualization purpose, the center point of each polar gain pattern in Fig. 4 and Fig. 5 is displaced to suggest the physical layout of the antenna elements. In each figure, the reference point O represents the center of the loop antenna. The gain pattern for the left dipole antenna is shifted in the negative **x** direction, such that the center of the left-dipole gain pattern falls on top of the physical center of the left dipole. Similarly, the gain pattern for the top dipole is shifted in the positive **y** direction, such that

the center of the top dipole gain pattern falls on the antenna's physical center. Thus, in the azimuth plane (where the perspective is from above, opposite the **z** axis), the gain pattern of the loop antenna is centered at the origin O of the antenna array, the gain pattern of the left antenna is to the left of O, and the gain pattern of the top antenna is above O. Similarly, in Fig. 5, the perspective is from the side (along the y axis), so the gain patterns of the loop antenna and the top dipole are both centered on the origin O and the gain pattern of the left dipole is to the left of O.

In the analysis that follows, only three of the five antenna elements will be analyzed. Specifically, to simplify the analysis, only the top dipole, the left dipole, and the small loop dipole are chosen to calculate the radiation pattern, which is numerically calculated with the increments of both azimuth angle ϕ, and elevation angle θ to be 1 degree. Assuming the distance between signal transmitter and the receiving AoA sensor is further away than the gap between two parallel short dipoles, the signals received by two parallel dipoles are supposed to have the same signal power. In this sense, the bottom and right antennae provide redundant information.

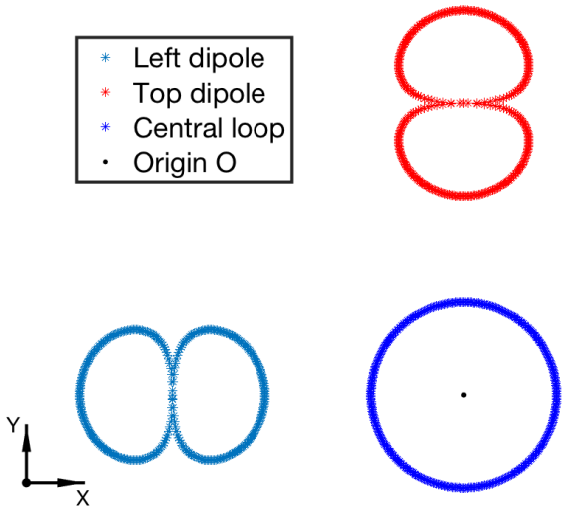

Fig. 4. Azimuth plane pattern. The symmetric gain of the loop antenna is 1.77 dBi.

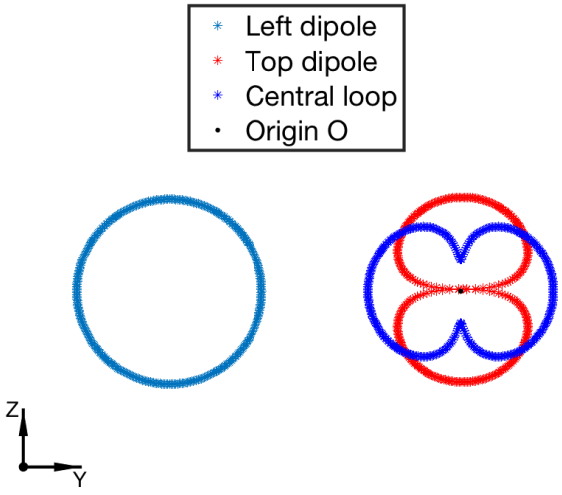

Fig. 5. Elevation plane pattern. The symmetric gain of the left antenna is 1.76 dBi.

The radiation patterns shown in Fig. 4 provide a more precise description of how the azimuth angle of the transmitter can be inferred by comparing received powers on different antenna elements. First, assume that the transmit antenna is in the far field,

such that the broadcast power incident on all the antenna elements is essentially equal. Given this assumption, the received power at each feeder is modulated primarily by the radiation pattern of each antenna element. As shown in the figure, if the transmitter's azimuth angle changes (without it leaving the plane), then the gain for one of the dipoles increases and, for the other dipole decreases. If the gain pattern equations can be inverted, then the measured gains on each antenna element can be mapped to an azimuth angle.

The radiation pattern shown in Fig. 5 provides additional insight about inferring the elevation angle. The figure indicates clearly that the loop antenna has a null along the vertical (**z** axis) while the top dipole has a null in the normal direction (**x** axis); hence elevation angle can be inferred by comparing the measured gains from the dipole antennae to those for the loop.

In reality, the gain patterns are 3D, so the azimuth and elevation angles must be computed simultaneously by inverting the full 3D gain pattern to extract AoA from signal powers obtained on the feeders for each of the antenna elements. A look-up table algorithm for solving this inverse problem is discussed in the following section.

It is important to note that the proposed array design has eight-way symmetry. This is to say that the mapping from angle to power is symmetric in the four quadrants of the azimuth plane and also symmetric above and below the azimuth plane. In other words, the angle-to-power relationships repeat for each octant of a three-dimensional grid with its origin at the loop antenna's center. For our application. We will assume that the ambiguity can be resolved from context (e.g. a first responder approaching a known building from a known direction can trivially identify the relevant solution out of the eight symmetric possibilities).

Estimation Algorithm

A look-up table approach is proposed as a means of inverting the radiation pattern to estimate the desired states from the measured observables. In this case, the desired states include the azimuth and elevation angles (θ, ϕ), whereas the measured observables include the measured power for the top dipole, the left dipole and the central loop antennas are (P_1, P_2, P_3). The observed powers are related to the antenna gains for the top dipole, the left dipole and the central loop antennas (G_1, G_2, G_3) through the signal power P_r incident on the array. The gain themselves are the functions of the AoA parameters of the incoming signal (θ, ϕ).

$$P_1 = P_r G_1(\theta, \phi) \quad (1)$$
$$P_2 = P_r G_2(\theta, \phi) \quad (2)$$
$$P_3 = P_r G_3(\theta, \phi) \quad (3)$$

The corresponding three signal magnitudes are the amplitudes of voltage signals measured on each antenna in the absence of noise.

$$M_1 = \sqrt{P_1} = \sqrt{P_r G_1} \quad (4)$$
$$M_2 = \sqrt{P_2} = \sqrt{P_r G_2} \quad (5)$$
$$M_3 = \sqrt{P_3} = \sqrt{P_r G_3} \quad (6)$$

In concept, a look-up table could be formulated by evaluating the three signal magnitudes (M_1, M_2, M_3) over a grid of the three state variables $(\theta, \phi, \mathrm{P_r})$; by inverting these formulae, it would be possible to obtain the three states from the three magnitude observables.

Note that the right and bottom dipoles are not specifically identified here, since these dipoles provide redundant information. In other words, the radiation patterns for the top and bottom antennae are both G_1, and for the right and left antennae are both G_2. In the future, this redundant information will be exploited for noise reduction; however, the redundant dipoles will be neglected here for the sake of simplicity.

Further simplification is possible by eliminating the incident power $\mathrm{P_r}$, which is a nuisance variable for this application. To eliminate the nuisance variable, all three magnitude observables can be normalized by their root-sum-squared M_c. The resulting normalized variables (M_4, M_5, M_6) are defined below.

$$M_c = \sqrt{M_1^2 + M_2^2 + M_3^2} = \sqrt{P_r(G_1 + G_2 + G_3)} \quad (7)$$

$$M_4 = \frac{M_1}{M_c} = \sqrt{\frac{G_1}{G_1 + G_2 + G_3}} \quad (8)$$

$$M_5 = \frac{M_2}{M_c} = \sqrt{\frac{G_2}{G_1 + G_2 + G_3}} \tag{9}$$

$$M_6 = \frac{M_3}{M_c} = \sqrt{\frac{G_3}{G_1 + G_2 + G_3}} \tag{10}$$

Importantly, the received signal power P_r is cancelled out when normalizing by M_c. Moreover, any one of the normalized variables can be computed from the other two. For instance:

$$M_6^2 = 1 - M_4^2 - M_5^2 \tag{11}$$

In our simulated implementations, the look-up table was constructed by evaluating the three radiation-pattern magnitudes $(\sqrt{G_1}, \sqrt{G_2}, \sqrt{G_3})$ over a grid of the AoA parameters (θ, ϕ), discretized with one-degree increments. Each pair of AoA parameters can be assigned an index k, and the set of all indices can be labeled K. Models of the normalized signal magnitude $(M_{u,k}, M_{v,k}, M_{w,k})$ can then be constructed using the following equations for each index k.

$$M_{t,k} = \sqrt{\left(\sqrt{G_{1,k}}\right)^2 + \left(\sqrt{G_{2,k}}\right)^2 + \left(\sqrt{G_{3,k}}\right)^2} = \sqrt{G_{1,k} + G_{2,k} + G_{3,k}} \tag{12}$$

$$M_{u,k} = \frac{\sqrt{G_{1,k}}}{M_{t,k}} \tag{13}$$

$$M_{v,k} = \frac{\sqrt{G_{2,k}}}{M_{t,k}} \tag{14}$$

$$M_{w,k} = \frac{\sqrt{G_{3,k}}}{M_{t,k}} \tag{15}$$

The look-up table can then be organized as a list of pairs $\{M_{u,k}, M_{v,k}, M_{w,k}\}$, each corresponding to a particular set of AoA parameters. Ideally the matched entry should make $M_4 = M_{u,k}, M_5 = M_{v,k}, M_6 = M_{w,k}$, so the best estimate corresponds to the index for which with the minimum value of $\left(M_4 - M_{u,k}\right)^2 + \left(M_5 - M_{v,k}\right)^2 + \left(M_6 - M_{w,k}\right)^2$. In other words, the look-up table provides the estimated AoA parameters $\{\hat{\theta}, \hat{\phi}\}$ by solving the following equation.

$$\{\hat{\theta}, \hat{\phi}\} = \underset{k \in K}{\operatorname{argmin}} \left(\left(M_4 - M_{u,k}\right)^2 + \left(M_5 - M_{v,k}\right)^2 + \left(M_6 - M_{w,k}\right)^2\right) \tag{16}$$

In implementing this look-up table, two important details must be considered. Specifically, the look-up table must both address the eight-way ambiguity issue and the potential issue in which more than one index in the table have the same associated observables (for example, due to roundoff error).

To address the issue of ambiguity, the grid of possible angles was defined to include only one octant of the full space of possible angles. In other words, the look-up table is constructed on the range of $\theta \in [0,90]$, and $\phi \in [0,90]$. As long as the target can be operationally confined to a single quadrant, then the solution is unambiguous; designing an algorithm for disambiguation will be left to the future work.

To address the issue of multiple grid indices with similar or identical observables, sets of similar observables were identified and clustered. The AoA parameters for all indices in the cluster were then set to the average value for the cluster. In effect, the clustering process joined multiple small grid cells with similar gain patterns into one larger grid cell, described by its centroid.

SYSTEM PERFORMANCE

The accuracy of the proposed AoA sensor is a strong function of ambient noise. Because the precise level of noise for any application (e.g. the first-responder application) is somewhat difficult to characterize in advance, a sensitivity study was conducted to simulate sensor accuracy as a function of signal-to-noise ratio (SNR).

In conducting such a sensitivity study, the nature of the noise source must be carefully defined. For instance, a directional noise source (from an external transmitter at a particular bearing angle) would result in correlated errors across antenna elements. By

contrast, internal thermal noise (e.g. noise introduced by amplifiers) will likely be independent between elements. The simulations in this section consider the latter case, where the noise on each element is independent. The noise is modeled most accurately in the voltage domain. Assuming the received signal magnitude observables imposed with noises are $(M_1 + N_1, M_2 + N_2, M_3 + N_3)$, three normalized magnitude observables (M_4, M_5, M_6) become

$$M_c = \sqrt{(M_1 + N_1)^2 + (M_2 + N_2)^2 + (M_3 + N_3)^2} \tag{17}$$

$$M_4 = \frac{M_1 + N_1}{M_c} \tag{18}$$

$$M_5 = \frac{M_2 + N_2}{M_c} \tag{19}$$

$$M_6 = \frac{M_3 + N_3}{M_c} \tag{20}$$

In this paper, the sensor noises (N_1, N_2, N_3) are assumed to be Gaussian, which means $N_u \sim N(0, \delta^2)$, where $u = 1,2, or\ 3$. It is assumed that the noise is the output of signal processing (e.g. correlation, etc.) Noise standard deviation δ may vary for different hardware configurations, for different waveform designs, and in different signal propagating environments. Defining SNR in dB scale as the ratio of the received signal power and the noise variance gives

$$SNR = 10 \log(P_r/\delta^2)\ . \tag{21}$$

The signal noise deviation under different SNRs can thus be represented as

$$\delta = \sqrt{\frac{P_r}{10^{\frac{SNR}{10}}}}\ . \tag{22}$$

The system performance of the proposed AoA sensor is investigated under different SNRs ranging from 30 dB to 50 dB with an interval of 2 dB. Three signal magnitude measurements are simulated as the sum of the perfect observables read from the look-up table and the noises generated under certain SNR in (22). Monte Carlo simulations are conducted here by compiling 500 trials, each comparing all possible azimuth and elevation truth (θ, ϕ) with noisy observables. The look-up table method outputs the estimated azimuth and elevation angles $(\hat{\theta}, \hat{\phi})$. Then the azimuth and elevation errors compared with the true values $(\theta - \hat{\theta}, \phi - \hat{\phi})$ can be easily obtained. Instead of dividing errors into azimuth and elevation parts, only one angle between the direction estimate and the true direction is adopted as the error metric. This is because the azimuth angle error is poorly defined near the poles. The unified angle error Ω between the estimated direction $(\hat{\theta}, \hat{\phi})$ and the truth (θ, ϕ) in spherical coordinates is computed by the following equations.

$$\overrightarrow{D_{true}} = (\sin(\theta) * \cos(\phi), \sin(\theta) * \sin(\phi), \cos(\theta)) \tag{23}$$

$$\overrightarrow{D_{est}} = \left(\sin(\hat{\theta}) * \cos(\hat{\phi}), \sin(\hat{\theta}) * \sin(\hat{\phi}), \cos(\hat{\theta})\right) \tag{24}$$

$$\Omega = \cos^{-1} \frac{\overrightarrow{D_{true}} \cdot \overrightarrow{D_{est}}}{|\overrightarrow{D_{true}}||\overrightarrow{D_{est}}|} \tag{25}$$

Simulations indicate that the angle error varies with the direction of signal arrival. AoA error distribution with SNR equal to 42 dB is shown in Fig. 6 and Fig. 7. Fig. 6 shows an isometric view of the error surface obtained from the Monte Carlo simulations. Fig. 7 shows a top view. Each point is the average-absolute-error for a particular angle of arrival. The concave shape of the error surface indicates that the proposed AoA sensor has better accuracy at medium azimuth and elevation angles. As expected, the error surface is symmetric in azimuth, but asymmetric in elevation (for angles above the plane of the antenna elements).

The average error over the whole error surface (for SNR equal to 42 dB) is 1.7 degrees. Whereas the error is as high as 3 degrees on the edges of the error surface, the error is below 1 degree in the middle of the domain. This accuracy, at least at the center of the error surface, is compatible with the requirements for the proposed first-responder scenario.

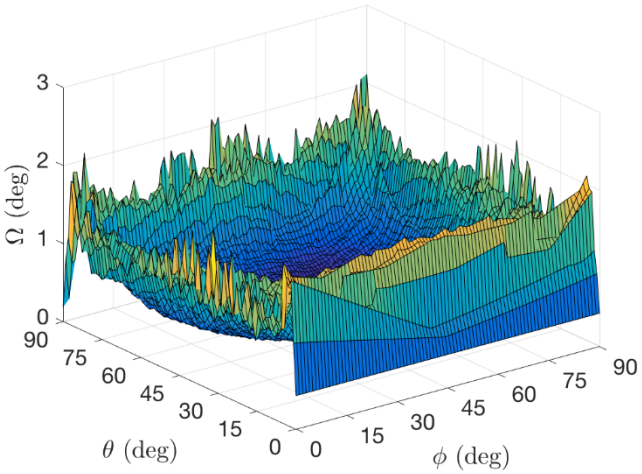

Fig. 6. AoA average-absolute-error with 42 dB SNR

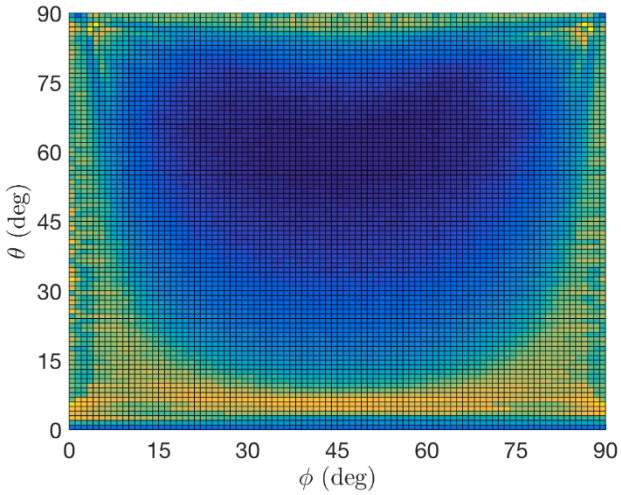

Fig. 7. Top view of error surface

The 42 dB case lies roughly in the middle of the range of SNR values simulated. Error values (averaged over the error surface) are shown for a range of different SNR values in Fig. 8. Averaging AoA error decreases as SNR increases. Simulations indicate that average AoA errors vary from 4.5 degrees (at 30 dB SNR) to 0.7 degrees (at 50 dB SNR).

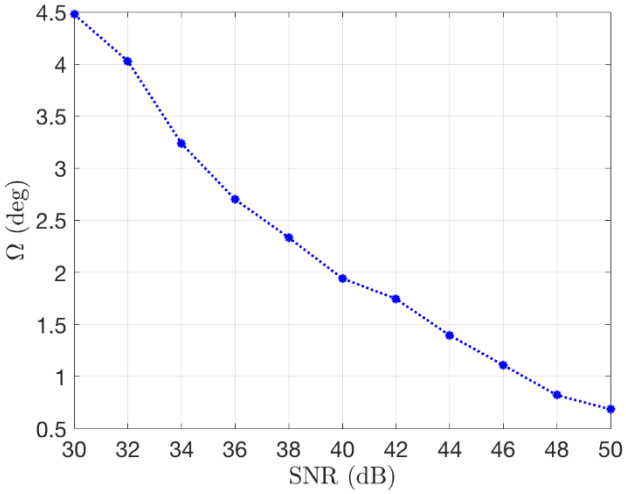

Fig. 8. AoA errors with different SNRs

CONCLUSIONS

This paper explores a novel AoA sensor designed as a flat radio antenna array composed of basic dipole and loop antenna elements. The proposed design is compact and lightweight. A look-up table method was proposed to map signal magnitude (power) observables from each element into an angle estimate. Initial simulation results show that the proposed sensor can provide 3D AoA measurement with an average-absolute-error over all directions of approximately 1.7 degrees for a nominal SNR of 42 dB (after signal processing).

ACKNOWLEDGMENTS

The author would like to express his gratitude to Prof. Jason Rife for his helpful advisory and comments. Also, the author would like to thank the China Scholarship Council for the financial support of this research.

REFERENCES

[1] Mukhopadhyay, Mainak, Binay Kumar Sarkar, and Ajay Chakraborty, "Augmentation of anti-jam GPS system using smart antenna with a simple DOA estimation algorithm," *Progress In Electromagnetics Research,* Vol. 67, 2007, pp. 231-249.

[2] Ellingson, Steven W, "Design and evaluation of a novel antenna array for azimuthal angle-of-arrival measurement," *IEEE Transactions on Antennas and Propagation,* Vol. 49, No. 6, 2001, pp. 971-979.

[3] Sanudin, Rahmat, "Planar array design and analysis on direction of arrival estimation for mobile communication systems," 2014.

[4] Dersan, Aysegul, and Yalcin Tanik, "Passive radar localization by time difference of arrival," In *MILCOM 2002. Proceedings*, Vol. 2, pp. 1251-1257. IEEE, 2002.

[5] Hartman, Richard L., Michael K. Balch, and Stephen R. Granade. "Wide angle laser range and bearing finder." U.S. Patent 7,345,743, issued March 18, 2008.

[6] Tooley, Michael H., and David Wyatt, *Aircraft communications and navigation systems: principles, operation and maintenance*. Routledge, 2007.

[7] Stutzman, Warren L., and Gary A. Thiele, *Antenna theory and design*. John Wiley & Sons, 2012, pp. 36-37.

[8] Van Veen, Barry D., and Kevin M. Buckley. "Beamforming: A versatile approach to spatial filtering." *IEEE assp magazine,* Vol. 5, No. 2, 1988, pp. 4-24.

[9] Schmidt, Ralph, "Multiple emitter location and signal parameter estimation," *IEEE transactions on antennas and propagation,* Vol. 34, No. 3, 1986, pp. 276-280.

[10] Roy, Richard, and Thomas Kailath, "ESPRIT-estimation of signal parameters via rotational invariance techniques," *IEEE Transactions on acoustics, speech, and signal processing,* Vol. 37, No. 7, 1989, pp. 984-995.

[11] Rife, Jason, "Convergence of Distributed Localization With Alternating Normals," *IEEE Transactions on Robotics,* Vol. 32, No. 5, 2016, pp. 1280-1284.

[12] Burke, Gerald J., A. J. Poggio, J. C. Logan, and J. W. Rockway, "Numerical electromagnetic code (NEC)," In *Electromagnetic Compatibility, 1979 IEEE International Symposium*, pp. 1-3. IEEE, 1979.